Journal of Clinical Monitoring and Computing (2020) 34:903–911
https://doi.org/10.1007/s10877-019-00402-z

ORIGINAL RESEARCH

Noninvasive measurement of stroke volume changes in critically ill patients by means of electrical impedance tomography

Fabian Braun[1,2] · Martin Proença[1,2] · Anna Wendler[3] · Josep Solà[1] · Mathieu Lemay[1] · Jean-Phillipe Thiran[2,4] · Norbert Weiler[3] · Inéz Frerichs[3] · Tobias Becher[3]

Received: 24 April 2019 / Accepted: 10 October 2019 / Published online: 17 October 2019

Abstract
Previous animal experiments have suggested that electrical impedance tomography (EIT) has the ability to noninvasively track changes in cardiac stroke volume (SV). The present study intended to reproduce these findings in patients during a fluid challenge. In a prospective observational study including critically ill patients on mechanical ventilation, SV was estimated via ECG-gated EIT before and after a fluid challenge and compared to transpulmonary thermodilution reference measurements. Relative changes in EIT-derived cardiosynchronous impedance changes in the heart (ΔZ_H) and lung region (ΔZ_L) were compared to changes in reference SV by assessing the concordance rate (CR) and Pearson's correlation coefficient (R). We compared 39 measurements of 20 patients. ΔZ_H did not show to be a reliable estimate for tracking changes of SV (CR = 52.6% and R = 0.13 with P = 0.44). In contrast, ΔZ_L showed an acceptable trending performance (CR = 94.4% and R = 0.72 with P < 0.0001). Our results indicate that ECG-gated EIT measurements of ΔZ_L are able to noninvasively monitor changes in SV during a fluid challenge in critically ill patients. However, this was not possible using ΔZ_H. The present approach is limited by the influences induced by ventilation, posture or changes in electrode–skin contact and requires further validation.

Keywords Noninvasive · Stroke volume · Cardiac output · EIT · Bioimpedance · Fluid challenge

1 Introduction

Fluid resuscitation is one of the vital components of hemodynamic management in critically ill patients. To ensure adequate tissue perfusion it should be targeted by optimizing cardiac stroke volume (SV) while limiting increases in filling pressures and development of edema. To achieve this goal, absolute values of SV and cardiac output are less important than monitoring trends in response to interventions such as a fluid challenge [1]. Therefore, continuous monitoring of changes in SV during fluid resuscitation is desirable.

Pulmonary artery catheterization (PAC) is an invasive method that provides continuous assessment of cardiac output in critically ill patients. However, due to the high risk for complications and questionable clinical benefit, PAC use is declining in clinical practice [2]. Transpulmonary thermodilution (TPTD) cardiac output with continuous monitoring by pulse contour analysis is a clinically established, and potentially less invasive, alternative [3]. Even though TPTD with pulse contour analysis is less invasive than PAC, it still requires placement of the central venous and peripheral arterial lines, and provides continuous data with limited reliability, requiring frequent re-calibration [4].

Thoracic electrical impedance tomography (EIT) is a noninvasive imaging modality providing real-time data on changes of electrical bioimpedance [5]. EIT can be used to track changes in pulmonary air content [6, 7] and, when used and interpreted in conjunction with a specific ventilator protocol, recruitment and derecruitment as well as relative hyperdistension [8, 9]. As pulsatile cardiovascular activity generates measurable changes in bioimpedance in the

✉ Fabian Braun
fbn@csem.ch

1 Centre Suisse d'Electronique et de Microtechnique (CSEM SA), Rue Jaquet-Droz 1, 2002 Neuchâtel, Switzerland

2 Signal Processing Laboratory LTS5, Swiss Federal Institute of Technology in Lausanne (EPFL), Lausanne, Switzerland

3 Department of Anesthesiology and Intensive Care Medicine, University Medical Center Schleswig-Holstein, Campus Kiel, Kiel, Germany

4 Department of Radiology, University Hospital Center and University of Lausanne, Lausanne, Switzerland

heart and lung regions, it has been presumed that EIT could be able to noninvasively track changes in SV, potentially making it a valuable monitoring tool for patients in need of hemodynamic optimization.

Vonk-Noordegraaf et al. [10] were the first to report the measurement of SV by means of EIT via the cardiosynchronous impedance change in the heart region (ΔZ_H) in humans. In two recent studies this was further investigated in pigs. Pikkemaat and colleagues [11] revealed certain issues (sensitivity to heart displacement and lung volume) of the heart-based SV estimation which require further investigation. Even though not reported in [11], the same study also estimated SV via the cardiosynchronous impedance change in the lung region (ΔZ_L) with comparable results to the heart-based approach [12]. The approach of tracking SV by analyzing changes in ΔZ_L was then further studied by the group of da Silva Ramos [13] who showed that (1) assessment of trending relative SV changes is feasible while (2) estimating absolute SV values requires anthropometric calibration. As also discussed in [14], these partly contradictory findings from animal studies [11–13] are not conclusive about the use of cardiosynchronous impedance changes in the heart (ΔZ_H) or lung region (ΔZ_L) as noninvasive surrogate measures of SV.

As all the recent work on noninvasive assessment of SV via EIT is based on animal experiments, we intended to investigate the applicability of this method in patients in the intensive care unit (ICU) receiving a fluid challenge. In particular we tested the two hypotheses that either ΔZ_H or ΔZ_L can be used to assess changes in SV by means of EIT.

2 Methods

2.1 Study population, data acquisition and study protocol

Between August 2016 and December 2017, we performed a prospective observational study including critically ill mechanically ventilated patients requiring fluid administration as per clinical decision under monitoring with both EIT and TPTD cardiac output. Exclusion criteria were: age below 18 years, BMI of more than 35 kg/m^2, open lung injuries, instable injuries of spine or skull, metallic implants in the thorax region (e.g. cardiac pacemaker). The study was approved by the local Ethics Committee of the Medical Faculty of the Christian-Albrechts University Kiel, Germany (EC-Study-ID D486/16) and registered prior to patient enrollment at ClinicalTrials.gov (NCT02992002, Principal investigator: Tobias Becher, Date of registration: December 14, 2016). Due to the purely observational nature of the study, informed consent was waived by the ethics committee. Some results of this study unrelated to SV analysis have been previously published [15].

All measurements were performed in the ICU facilities of the University Medical Center Schleswig-Holstein (UKSH, Kiel, Germany). The patients were equipped with a 16-electrode EIT belt placed around their chest at the level of the 4th to 5th intercostal space and connected to the PulmoVista™ 500 EIT device (Dräger Medical, Lübeck, Germany). Hemodynamic data including ECG were measured using a Datex-Ohmeda hemodynamic monitor (S/5, Datex-Ohmeda, Helsinki, Finland) and recorded via the S/5 Collect software (Datex-Ohmeda, Helsinki, Finland). SV reference measurements were obtained by averaging three TPTD measurements performed with the PiCCO plus device (Pulsion, Munich, Germany). Figure 1 shows the schematic drawing of the measurement setup.

For the present analysis, SV reference values were obtained from repeated TPTD measurements at three different time points (M1 to M3): (M1) 30 min after application of the EIT belt and prior to the fluid challenge via the injection of 500 mL of balanced electrolyte solution (Sterofundin ISO, B. Braun, Melsungen, Germany); (M2) right after the fluid challenge; (M3) 30 min after (M2). For those patients being *fluid responsive*, an increase in SV of at least 15% was expected from (M1) to (M2). Moreover, if all of the injected liquid remained in the circulation, SVs of (M3) and (M2) were expected to be comparable.

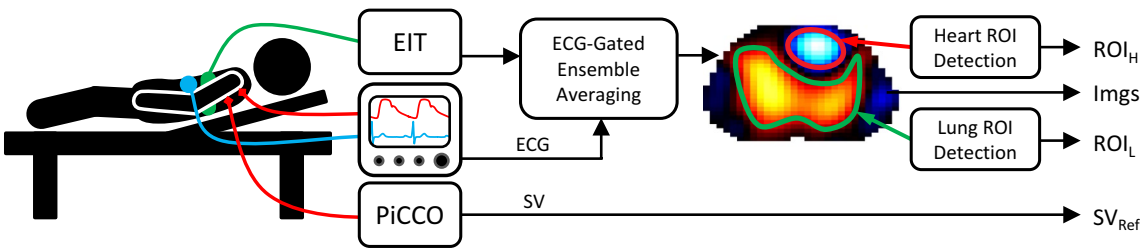

Fig. 1 Block diagram of the measurement setup. For each SV measurement the EIT images are averaged to one representative cardiac cycle (Imgs) from which regions of interest representing the heart (ROI_H) and lung regions (ROI_L) are extracted. The amplitudes of the temporal sum signals in these two regions are further compared to the SV reference measurement SV_{REF}

2.2 Data preprocessing

First, EIT and hemodynamic data were manually synchronized in the time domain with the help of deliberate spikes induced via synchronous tapping on EIT and ECG electrodes as detailed in [14]. All heartbeats in a 2 min window centered around the mean time of injection of the TPTD triplets were averaged via ECG-gated ensemble averaging to one representative cardiac cycle per measurement (M1 to M3) as further described in [14]. EIT raw voltages were reconstructed into sequences of images with 32×32 pixels using the GREIT algorithm [16] with the recommended parameters in combination with the 2.5D model of an adult human thorax available in the EIDORS toolbox [17]. Then, for each resulting EIT image sequence, regions of interest were determined as described in [14, 18] for the heart (ROI_H) and via the algorithm proposed in [19, 20] for the lungs (ROI_L). In brief, these algorithms exploit the amplitude and phase information of the EIT image sequence at the cardiac frequency to separate the heart from the lungs. The cardiosynchronous impedance changes in the heart and the lung regions both exhibit high amplitudes but of opposite phase, which are attributable to blood leaving the heart while the lungs are being filled with blood and vice versa. The resulting two regions of interest were then applied to separately analyze impedance changes in the heart (ROI_H) and lung (ROI_L) regions.

2.3 Signal processing and data analysis

As mentioned in the introduction, we tested two hypotheses: whether changes in SV can be assessed by means of EIT via the signal amplitude in either (a) the heart [10, 11] or (b) the lung region [12, 13]. To do so, the amplitudes ΔZ_H and ΔZ_L of the temporal sum signals in both ROI_H and ROI_L were estimated for each of the averaged EIT image sequences as the peak-to-peak amplitude of the corresponding temporal sum signal, i.e. the sum over all pixels in the corresponding region. To allow for a fair comparison between the three measurements (M1 to M3) of each patient, the abovementioned amplitudes were calculated from the same heart and lung regions which were averaged from the three individual regions of measurements at time points M1 to M3.

The SV trending ability of EIT was tested by transforming the two amplitude features (ΔZ_H and ΔZ_L) into relative changes between the current measurement c and a baseline measurement b: $\Delta SV_{EIT}^{b\to c} = \left(\Delta Z_X^c - \Delta Z_X^b\right)/\Delta Z_X^b$, where ΔZ_X represents ΔZ_H or ΔZ_L. The reference measurements SV_{Ref} were transformed similarly and denoted as ΔSV_{Ref}.

As further explained in the results and discussion sections, the relative changes of the two transitions M1 to M2 and M2 to M3 were tested for each patient, i.e. $\Delta SV_{Ref}^{M1\to M2}$ versus $\Delta SV_{EIT}^{M1\to M2}$ and $\Delta SV_{Ref}^{M2\to M3}$ versus $\Delta SV_{EIT}^{M2\to M3}$ were compared by means of four-quadrant plot analysis [21, 22]. The resulting trending performance was evaluated by means of the concordance rate CR (percentage of data points lying in the 1st and 3rd quadrant, as thoroughly discussed in [21, 22] and Pearson's correlation coefficient R. According to the criteria defined by Critchley [21] trending performance was considered as acceptable if $CR \geq 92\%$. Variations of ΔSV_{Ref} and ΔSV_{EIT} below $\pm 13\%$ were excluded from four-quadrant plot analysis (exclusion zone) as this is the error to be expected from averaging a triplet of TPTD measurements [23, 24].

In a second analysis the relative SV changes were transformed into absolute SV values by using one TPTD measurement as calibration, i.e. SV_{EIT}^{M1} and SV_{EIT}^{M3} (expressed in mL) were obtained by calibrating $\Delta SV_{EIT}^{M1\to M2}$ and $\Delta SV_{EIT}^{M2\to M3}$ against SV_{Ref}^{M2}. The noninvasive estimates SV_{EIT}^{M1} and SV_{EIT}^{M3} were then compared to SV_{Ref}^{M1} and SV_{Ref}^{M3} by means of Bland–Altman analysis.

2.4 Rejection of outliers caused by variations in tidal volume ratio

It is known that changes in tidal volume (VT) correlate well with changes in global EIT impedance [25, 26]. Therefore, the ratio of EIT-derived VT versus true—ventilator-derived—VT should remain constant over time if no perturbation (such as EIT belt displacement or EIT electrode contact problem) occurred. As such perturbations can also impair the EIT-based hemodynamic parameter estimation, potential outliers were identified and removed from the analysis. To this end, for each measurement (M1 to M3), VT was estimated in two ways: (a) from the ventilator data provided to the EIT machine via the MEDIBUS interface (VT_V) and (b) as the sum of all pixels of a functional ventilation image (standard-deviation in the temporal domain) obtained from band-pass filtered (cutoff frequencies: [0.1, 0.5] Hz) EIT images (VT_E). Then the ratio of these VT was calculated as $VT_{E/V} = VT_E/VT_V$. For each relative measurement M1 to M2 and M2 to M3 the relative change in this tidal volume ratio was calculated as follows: $\Delta VT_{E/V}^{M1\to M2} = \left(VT_{E/V}^{M2} - VT_{E/V}^{M1}\right)/VT_{E/V}^{M1}$ and $\Delta VT_{E/V}^{M2\to M3} = \left(VT_{E/V}^{M3} - VT_{E/V}^{M2}\right)/VT_{E/V}^{M2}$, respectively. The analysis was restricted to measurements which fell into the limits of the 95% confidence interval, i.e. $\mu_{\Delta VT_{E/V}} - 1.96\sigma_{\Delta VT_{E/V}} < \Delta VT_{E/V} < \mu_{\Delta VT_{E/V}} + 1.96\sigma_{\Delta VT_{E/V}}$, with $\mu_{\Delta VT_{E/V}}$ and $\sigma_{\Delta VT_{E/V}}$ as the mean and standard-deviation of all $\Delta VT_{E/V}$.

3 Results

In total, 25 patients were included in the study. The average duration of fluid administration was 15 ± 6 (range: 5–28) minutes. 12 out of 25 patients were "fluid responsive", as

defined by an increase in SV of more than 15% after fluid administration.

Since no ECG signal was recorded in the first four patients, only 21 out of 25 patients (15 male/6 female, age: 59 ± 22 years, weight: 78 ± 12 kg, height: 175 ± 7, BMI: 25 ± 3 kg/m^2, denoted as P5 to P25) were included in the present analysis. Due to technical issues with the EIT device the last measurement (M3) of subject P21 was not recorded and therefore only $\Delta SV_{EIT}^{M1\rightarrow M2}$ and $\Delta SV_{SV}^{M1\rightarrow M2}$ were compared for this subject. Finally, the measurements of P25 were removed from further analysis since the variations in tidal volume ratios $\Delta VT_{E/V}$ exceeded the 95% limits defined by the outlier removal approach. This results in a total of 39 measurements performed in 20 patients remaining for analysis, including 9 fluid "responders" and 11 "non-responders". Table 1 shows ventilation parameters and SV reference measurements for each patient.

3.1 Hemodynamic variations

The average changes in SV_{Ref} between the three measurements (M1, M2 and M3) were as follows: the fluid challenge generally led to an increase of SV (M2 vs. M1: $\Delta SV_{Ref}^{M1\rightarrow M2} = 13.1\%$) while 30 min after SV returned to its baseline level (M2 vs M3: $\Delta SV_{Ref}^{M2\rightarrow M3} = -10.0\%$). Relative changes in SV and $\Delta VT_{E/V}$ and the EIT-derived amplitudes ΔZ_H and ΔZ_L are listed in Table 2 for each patient.

3.2 SV trending performance of EIT

The trending performance for all 39 measurements and the two EIT-based amplitude features (ΔZ_H and ΔZ_L) is shown in Fig. 2a and b by means of four-quadrant plot analysis. CR of 52.6% and R of 0.13 (P = 0.44) were obtained for the heart-related amplitude ΔZ_H (Fig. 2a). In contrast, using the lung-related amplitude ΔZ_L led to CR of 94.4% and R of 0.72 (P < 0.0001) as shown in Fig. 2b.

3.3 Absolute SV measurements after calibration

Assuming a calibration with TPTD at the time of measurement M2, absolute SV values were obtained for measurements M1 and M3. The comparison of invasive measurements SV_{Ref}^{M1} and SV_{Ref}^{M3} versus noninvasive estimates SV_{EIT}^{M1} and SV_{EIT}^{M3} is shown in Fig. 2c and d by means of

Table 1 Ventilation and hemodynamic parameters for each measurement (M1 to M3) and each patient (P05 to P25)

	PEEP (mbar)	ΔPinsp (mbar)	Ventilator mode	FiO2 (%)			Tidal volume (mL)			Noradrenaline (µg/kg/min)			Stroke volume (mL)		
	M1 to M3	M1 to M3	M1 to M3	M1	M2	M3	M1	M2	M3	M1	M2	M3	M1	M2	M3
P05	8	15	PCV	30	30	30	660	653	654	0.084	0.074	0.074	106	117	110
P06	8	15	PCV	30	30	30	529	529	545	0.201	0.203	0.203	113	111	113
P07	7	16	PCV	30	30	30	458	434	472	0.381	0.381	0.381	60	78	59
P08	10	22	PCV	50	50	50	660	642	655	0.108	0.108	0.108	136	130	129
P09	9	12	PSV	40	40	40	439	414	410	0.183	0.183	0.183	60	64	55
P10	8	20	PCV	30	30	30	586	565	571	1′078	1′078	1′078	105	110	108
P11	9	18	PCV	40	40	40	797	782	787	0.084	0.084	0.021	76	83	79
P12	9	13	PSV	35	35	35	673	776	686	0.080	0.000	0.080	126	131	119
P13	8	15	PCV	60	60	50	500	487	487	0.147	0.107	0.147	62	71	71
P14	10	10	PCV	35	35	35	1088	1037	986	0.356	0.356	0.356	87	119	75
P15	10	12	PSV	30	30	30	806	1069	1050	0.400	0.400	0.400	62	72	59
P16	7	5	PSV	30	30	30	868	797	863	0.175	0.175	0.150	67	70	68
P17	6	14	PCV	30	30	30	641	635	642	0.227	0.200	0.200	85	107	92
P18	5	12	PSV	45	45	45	554	614	536	0.038	0.038	0.038	54	54	52
P19	8	19	PCV	30	30	30	480	460	445	0.066	0.003	0.058	75	80	72
P20	8	14	PCV	35	35	35	654	640	631	0.257	0.257	0.257	58	68	64
P21	7	13	PCV	45	45	45	500	441	492	0.304	0.304	0.286	65	71	71
P22	5	14	PCV	35	35	35	480	440	461	0.013	0.013	0.013	57	81	64
P23	11	15	PCV	60	60	60	552	526	570	0.213	0.213	0.213	99	100	86
P24	10	15	PCV	45	45	45	530	517	505	0.188	0.111	0.111	47	57	50
P25	7	11	PCV	50	50	50	536	457	541	0.333	0.333	0.333	71	84	74

PEEP positive end-expiratory pressure, Δ*Pinsp* inspiratory pressure above PEEP for PCV and level of pressure support for PSV, *PCV* pressure controlled ventilation, *PSV* pressure support ventilation, *FiO2* fraction of inspired oxygen

Table 2 Relative changes of reference stroke volume (ΔSV_{Ref}) and EIT-derived parameters between measurements M1 and M2 and M2 and M3, denoted as M1 → M2 and M2 → M3, respectively

	ΔSV_{Ref} (%)		ΔSV_{EIT} via ΔZ_H (%)		ΔSV_{EIT} via ΔZ_L (%)		$\Delta VT_{E/V}$ (%)	
	M1 → M2	M2 → M3	M1 → M2	M2 → M3	M1 → M2	M2 → M3	M1 → M2	M2 → M3
P05	10.7	−6.3	0.8	4.8	13.9	−9.2	−6.7	3.1
P06	−1.0	1.1	−11.0	1.9	7.5	−7.6	−3.9	3.4
P07	29.9	−24.2	25.8	−16.1	26.5	−18.8	1.6	−0.3
P08	−4.5	−0.6	−7.2	3.1	−1.8	1.7	−3.0	−1.1
P09	7.6	−14.7	−32.2	28.7	22.4	−21.2	0.1	−5.7
P10	5.5	−2.1	−12.4	9.0	−7.7	1.3	−5.6	4.3
P11	9.4	−4.3	−2.8	12.7	3.9	−1.6	0.7	−0.1
P12	3.7	−8.6	10.9	−14.5	2.5	−10.5	−8.8	9.8
P13	9.3	2.1	−23.0	−0.5	14.6	2.6	−5.4	3.3
P14	13.7	−23.5	12.3	−6.1	14.1	−6.5	−3.5	8.7
P15	16.1	−18.3	17.6	−6.9	17.2	−4.3	−1.8	−2.2
P16	3.8	−2.6	−6.9	3.3	−6.6	−21.0	0.9	−5.3
P17	25.7	−14.1	−0.5	−0.9	14.8	−11.5	−0.4	−1.7
P18	0.3	−4.9	6.4	−1.1	−6.7	3.6	8.2	−2.7
P19	7.3	−10.3	1.1	−6.5	−3.4	−1.8	−16.9	−7.5
P20	9.7	0.0	−5.1	0.7	6.5	−5.2	−2.1	−1.0
P21	8.5	0.7	−30.9	*N/A*	17.8	*N/A*	−5.7	*N/A*
P22	43.3	−21.5	−5.8	7.3	16.4	−13.0	−2.2	−6.0
P23	0.6	−13.8	−44.1	19.0	−12.5	9.7	1.9	−7.4
P24	20.7	−12.0	33.4	−25.6	7.0	−10.4	−1.2	2.0
P25	18.0	−11.2	−41.7	58.4	−19.8	27.5	−30.7	23.5

Estimated stroke volume was determined via the heart amplitude ΔZ_H or lung amplitude ΔZ_L, and $\Delta VT_{E/V}$ as the ratio of tidal volume derived via EIT (VT_E) versus ventilator (VT_V). N/A indicates missing values due to technical issues with the EIT device

Bland–Altman analysis. For the heart-related amplitude ΔZ_H in Fig. 2c a bias of 11.9 mL and 95% limits of agreement (LOA) of −20.4 to 44.1 mL were obtained. The use of the lung-related amplitude ΔZ_L shown in Fig. 2d resulted in a bias of 2.7 mL and LOA of −12.3 to 17.6 mL.

4 Discussion

In the present study, we assessed EIT measurements performed before, during and after a clinically indicated fluid challenge for their ability to track changes in cardiac SV in critically ill adult patients. In particular, we analyzed the changes in cardiosynchronous impedance amplitudes in the heart and lung region and compared them to reference measurements obtained via TPTD. Analyzing the changes in heart-beat-related impedance amplitudes in the lung region, we found a high concordance rate of 94.4% and a strong correlation ($R = 0.72$ with $P < 0.0001$) with the reference measurements. Bland–Altman analysis revealed LOA of −12.3 to 17.6 mL with minimal bias. In contrast, our analysis of the cardiosynchronous impedance amplitudes in the heart region resulted in a weak correlation ($R = 0.13$ with $P = 0.44$) and LOA of −20.4 to 44.1 mL.

4.1 Hemodynamic variations

On average, SV increased most between M1 and M2 ($\Delta SV_{Ref}^{M1 \rightarrow M2} = 13.1\%$) and decreased most between M2 and M3 ($\Delta SV_{Ref}^{M2 \rightarrow M3} = -10.0\%$). This justifies our choice of analyzing the trending ability from M1 to M2 and from M2 to M3, in order to get the lowest possible amount of measurements falling within the error range of the reference device (i.e. the exclusion zone in the four-quadrant plot). On average, we observed only a slight increase in SV in response to the fluid challenge ($\Delta SV_{Ref}^{M1 \rightarrow M2} = 13.1\%$). This is due to the fact that only 9 out of 20 patients were "fluid responsive", as defined by a change in SV of > 15% after fluid challenge [27]. The subsequent return of SV to baseline could be explained by a redistribution of the crystalloid solution used for injection. A few minutes after the fluid challenge with crystalloids, only roughly 25% of the injected volume remains in the circulation [28], explaining the observed return of SV to its baseline level.

4.2 SV trending performance of EIT

As shown in Fig. 2a, the cardiosynchronous amplitude in the heart region, ΔZ_H, does not provide a reliable estimate

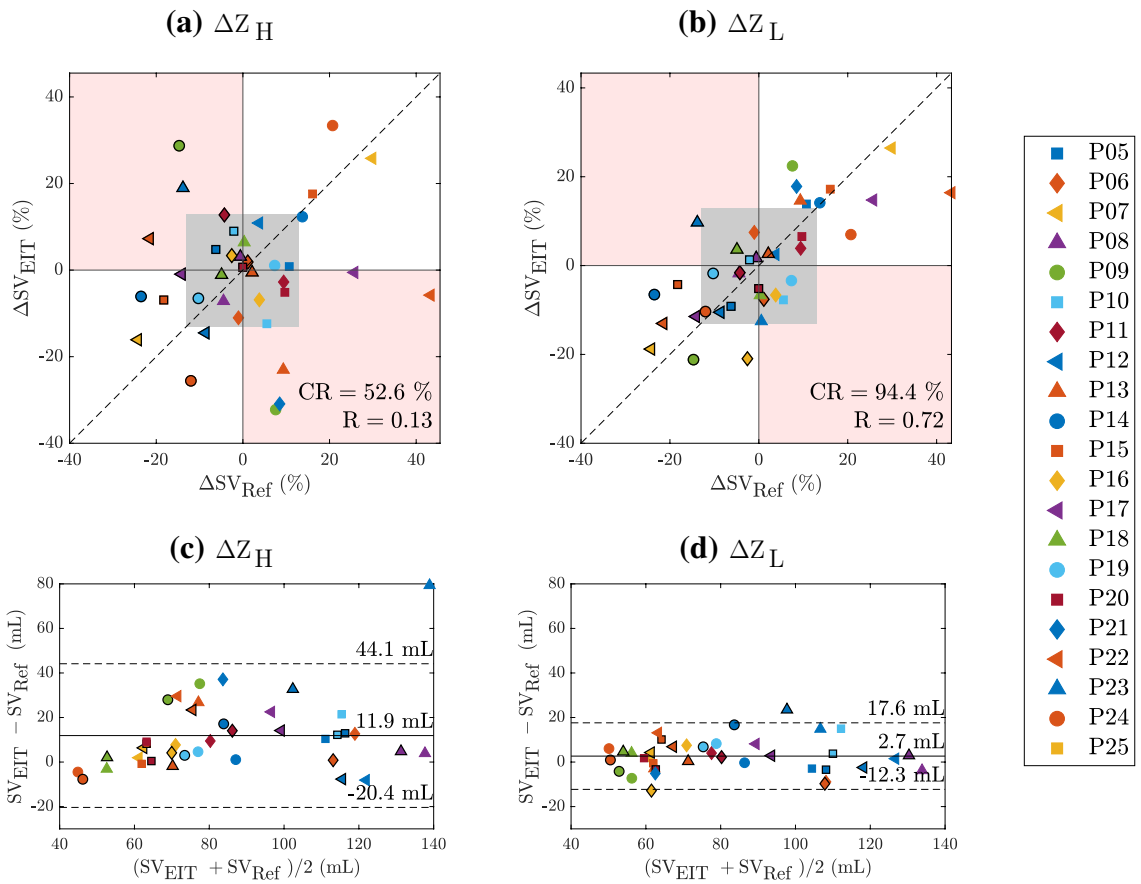

Fig. 2 **a** and **b**: Trending analyses between ΔSV_{EIT} versus ΔSV_{Ref} by means of four-quadrant plot analysis for **a** the heart amplitude ΔZ_H and **b** the lung amplitude ΔZ_L. The performance is assessed using the concordance rate CR and Pearson's correlation coefficient R. Each analysis includes a total of 39 measurement points (from 20 patients) representing relative changes from M2 to M3 (symbols with black border) and changes from M1 to M2 (symbols with no border). **c** and **d**: Bland–Altman analysis for **c** heart and **d** lung amplitude comparing SV^{M1}_{EIT} versus SV^{M1}_{Ref} (no border) and SV^{M3}_{EIT} versus SV^{M3}_{Ref} (with black border) after calibration against SV^{M2}_{Ref}

(CR = 52.6% and R = 0.13 with P = 0.44) for the noninvasive trending of SV via EIT. In contrast, the cardiosynchronous amplitude in the lung region, ΔZ_L, shown in Fig. 2b indicates an acceptable trending performance with CR = 94.4% and R = 0.72 (P < 0.0001).

Based on the present analysis we must reject the hypothesis that the EIT amplitude ΔZ_H can be used for trending—i.e. following relative changes—of SV, which is in contradiction with previous studies [10, 11]. We hypothesize that the heart-region-based SV estimation is strongly affected by the placement of the EIT belt with respect to the patient's heart or by ventilation-induced displacement of the heart. While in the animal experiments by Pikkemaat et al. [11] more accurate belt placements might have led to a less pronounced influence of the first effect in some pigs, it was still mentioned as a main limitation for other pigs [11].

In contrast, our analysis confirms that the EIT amplitude ΔZ_L can be successfully used for noninvasive trending of SV. However, this is only possible after exclusion of two measurements with high variations in tidal volume ratios $VT_{E/V}$. Without this exclusion a less good performance of CR = 85.0% and R = 0.54 (P < 0.001) was obtained (results not shown). This highlights the sensitivity of our approach to perturbations such as electrode–skin contact problems [29], EIT belt displacement [18] or large changes in ventilation [30]. Thus, contrary to the amplitude in the heart region, SV trending via the amplitude in the lung region might be more promising. This would confirm the recent work by da Silva Ramos and colleagues [13] but is at the same time partly in contradiction with the mixed results obtained by Pikkemaat [12]. Besides, these two studies [12, 13] were performed on pigs under laboratory conditions while our study is based on clinical data of ICU patients and thus reveals more challenges encountered under real-life conditions in a less controlled environment.

4.3 Limitations and future work

The present study is limited in various aspects. First, we could only analyze a total of 39 measurements from 20 patients with rather low variations in SV ($|\Delta SV_{Ref}| = 11.7 \pm 11.0\%$, range 0.1% to 43.3%). Even though a passive leg raising maneuver—instead of a fluid challenge—could lead to higher variations in SV, this is not common practice in this ICU due to practical considerations. As the current patient population contains many "non-responders" to fluid, enrolling more patients could increase the ΔSV and might also allow to only include those patients being fluid-responsive.

Second, our SV trending approach relies on the cardiosynchronous EIT amplitude in the lung region, which might suggest that ΔZ_L represents global perfusion, which is also a widespread assumption [31]. However, the cardiosynchronous EIT signals in the lung region do not necessarily precisely reflect pulmonary perfusion as discussed by Hellige and Hahn [32] and Adler et al. [33]. For example, two branches of pulmonary arteries with equal perfusion but different compliance would result in different cardiosynchronous EIT signal amplitudes [20]. Therefore, it is important to underline that our approach is not intended to detect regional pulmonary perfusion but rather investigates trends in cardiosynchronous impedance changes, as detected in the pulmonary region, to follow changes in cardiac SV. As shown in our Bland–Altman analysis, it can be calibrated using actual SV measurements. This procedure introduces a calibration factor that corrects for inter-individual variability of parameters like pulmonary artery compliance and therefore allows relatively accurate trending of actual SV. Of note, some patients were under high doses of vasopressors which may have an influence on pulmonary vascular resistance and may decrease hypoxic pulmonary shunt. Since we did not measure pulmonary arterial pressure in our study, we were not able to assess the actual impact of pulmonary vascular resistance on our findings. Nevertheless, it appears that our calibration procedure led to reliable estimations of changes in SV even in patients under high doses of vasopressors.

Even though the present approach shows promise on the current data, further research—including long-term measurements and patients with various pathophysiological conditions—is required to reveal possible limitations of this approach. Furthermore, the use of hypertonic saline injection as EIT contrast agent [34–36] could help to reveal potential discrepancies between the cardiosynchronous EIT signal in the lung region and the real pulmonary perfusion.

Third, since all patients were on pressure-controlled ventilation (PCV) or pressure support ventilation (PSV) we did not assess plateau pressure or static respiratory system compliance. Approximately one-third of patients had relevant spontaneous breathing activity, which makes calculation of compliance during PCV or PSV unreliable [37].

Fourth, the use of ECG-gated EIT averaging is not ideal in patients with cardiac arrhythmia. A more sophisticated method for isolating cardiosynchronous changes form the EIT images will be necessary in this group of patients.

Finally, it has also been shown in healthy volunteers that EIT-based SV estimation is sensitive to perturbations from electrode–skin contact problems or changes in posture [29]. The latter has also been reported for cardiac EIT signals in general [30, 38]. This might limit the present approach to scenarios where minimal changes in the EIT measurement setup occur (i.e. stable ventilation, stable electrode contact and unchanged posture).

For future studies, it might be of interest to investigate the trending capability in a patient population with higher intra-subject variations of SV (e.g. during hemorrhage or fluid resuscitation) and to assess the effects of different fluids (crystalloid, colloid, blood, etc.). Moreover, a specific protocol including different ventilation maneuvers would further allow to better identify the limitations of our approach related to changes in lung volume. Finally, the long-term trending performance of our noninvasive approach could also be compared to continuous pulse contour analysis with intermittent TPTD measurements.

5 Conclusion

In our study, we demonstrated the ability of EIT to assess changes in SV by analyzing cardiosynchronous impedance changes in the lung region. This approach is limited by the influences induced by ventilation, posture or electrode contact impedance. Future work should thus investigate potential limitations of this approach in detail. If it shows acceptable in certain situations, EIT could be a useful tool for noninvasive monitoring of SV trends at the bedside.

Funding FB was supported by the Swiss National Science Foundation Nano-Tera project OBESENSE (20NA21-1430801, http://www.nano-tera.ch). This study did not receive any external funding.

Compliance with ethical standards

Conflicts of interest TB has received consulting fees and lecture fees from Dräger Medical, Lübeck, Germany. IF reports reimbursement of speaking fees and travel costs from Dräger Medical, Lübeck, Germany. The other authors report no financial relationships relevant to this manuscript.

Ethical approval All procedures performed in studies involving human participants were in accordance with the ethical standards of the institutional research committee (Ethics Committee of the Medical Faculty of the Christian-Albrechts University Kiel, Germany, EC-Study-ID

D486/16) and with the 1964 Helsinki declaration and its later amendments or comparable ethical standards.

Informed consent Due to the purely observational nature of the study, informed consent was waived by the ethics committee.

References

1. Vincent J-L, De Backer D, Finfer SR, Vincent J-L. Circulatory shock. N Engl J Med. 2013;369:1726–34.
2. Wiener RS, Welch HG. Trends in the use of the pulmonary artery catheter in the United States, 1993-2004. JAMA [Internet]. 2007;298. http://jama.jamanetwork.com/article.aspx?doi=10.1001/jama.298.4.423. Accessed 12 Dec 2018.
3. De Backer D, Hajjar LA, Pinsky MR. Is there still a place for the Swan-Ganz catheter? We are not sure. Intensive Care Med. 2018;44:960–2.
4. Bein B, Meybohm P, Cavus E, Renner J, Tonner PH, Steinfath M, et al. The reliability of pulse contour-derived cardiac output during hemorrhage and after vasopressor administration. Anesth Analg. 2007;105:107–13.
5. Frerichs I, Amato MBP, van Kaam AH, Tingay DG, Zhao Z, Grychtol B, et al. Chest electrical impedance tomography examination, data analysis, terminology, clinical use and recommendations: consensus statement of the TRanslational EIT developmeNt stuDy group. Thorax. 2017;72:83–93.
6. Richard J, Pouzot C, Gros A, Tourevieille C, Lebars D, Lavenne F, et al. Electrical impedance tomography compared to positron emission tomography for the measurement of regional lung ventilation: an experimental study. Crit Care. 2009;13:R82.
7. Frerichs I, Hinz J, Herrmann P, Weisser G, Hahn G, Dudykevych T, et al. Detection of local lung air content by electrical impedance tomography compared with electron beam CT. J Appl Physiol. 2002;93:660–6.
8. Costa ELV, Borges JB, Melo A, Suarez-Sipmann F, Toufen C, Bohm SH, et al. Bedside estimation of recruitable alveolar collapse and hyperdistension by electrical impedance tomography. Intensive Care Med. 2009;35:1132–7.
9. Zick G, Elke G, Becher T, Schädler D, Pulletz S, Freitag-Wolf S, et al. Effect of PEEP and tidal volume on ventilation distribution and end-expiratory lung volume: a prospective experimental animal and pilot clinical study. Morty RE, editor. PLoS ONE. 2013;8:e72675.
10. Vonk Noordegraaf A, Janse A, Marcus JT, Bronzwaer JG, Postmus PE, Faes TJ, et al. Determination of stroke volume by means of electrical impedance tomography. Physiol Meas. 2000;21:285–93.
11. Pikkemaat R, Lundin S, Stenqvist O, Hilgers R-D, Leonhardt S. Recent advances in and limitations of cardiac output monitoring by means of electrical impedance tomography. Anesth Analg. 2014;119:76–83.
12. Pikkemaat R. Kardiopulmonales monitoring mit Hilfe der elektrischen Impedanztomographie [Internet]. Aachen, Germany: Shaker; 2015. http://d-nb.info/107591549X.
13. da Silva Ramos FJ, Hovnanian A, Souza R, Azevedo LCP, Amato MBP, Costa ELV. Estimation of stroke volume and stroke volume changes by electrical impedance tomography. Anesth Analg. 2018;126:102–10.
14. Braun F. Noninvasive stroke volume monitoring by electrical impedance tomography [Internet]. [Lausanne, Switzerland]: École Polytechnique Fédérale de Lausanne; 2018. http://dx.doi.org/10.5075/epfl-thesis-8343. Accessed 18 Apr 2017.
15. Becher T, Wendler A, Eimer C, Weiler N, Frerichs I. Changes in electrical impedance tomography findings of ICU patients during rapid infusion of a fluid bolus: a prospective observational study. Am J Respir Crit Care Med. 2019; in press.
16. Adler A, Arnold JH, Bayford R, Borsic A, Brown B, Dixon P, et al. GREIT: a unified approach to 2D linear EIT reconstruction of lung images. Physiol Meas. 2009;30:S35–55.
17. Adler A, Lionheart WR. Uses and abuses of EIDORS: an extensible software base for EIT. Physiol Meas. 2006;27:S25–42.
18. Braun F, Proença M, Lemay M, Bertschi M, Adler A, Thiran J-P, et al. Limitations and challenges of EIT-based monitoring of stroke volume and pulmonary artery pressure. Physiol Meas. 2018;39:014003.
19. Proença M, Braun F, Solà J, Adler A, Lemay M, Thiran J-P, et al. Non-invasive monitoring of pulmonary artery pressure from timing information by EIT: experimental evaluation during induced hypoxia. Physiol Meas. 2016;37:713–26.
20. Proença M. Non-invasive hemodynamic monitoring by electrical impedance tomography [Internet]. [Lausanne, Switzerland]: École Polytechnique Fédérale de Lausanne; 2017. http://dx.doi.org/10.5075/epfl-thesis-7444 Accessed 18 Apr 2017.
21. Critchley LA. Minimally invasive cardiac output monitoring in the Year 2012. In: Aronow WS, editor. Artery Bypass [Internet]. Rijeka, Croatia: InTech; 2013 http://www.intechopen.com/books/artery-bypass/minimally-invasive-cardiac-output-monitoring-in-the-year-2012 Accessed 18 Apr 2017.
22. Saugel B, Grothe O, Wagner JY. Tracking changes in cardiac output: statistical considerations on the 4-quadrant plot and the polar plot methodology. Anesth Analg. 2015;121:514–24.
23. Reuter DA, Huang C, Edrich T, Shernan SK, Eltzschig HK. Cardiac output monitoring using indicator-dilution techniques: basics, limits, and perspectives. Anesth Analg. 2010;110:799–811.
24. Stetz CW, Miller RG, Kelly GE, Raffin TA. Reliability of the thermodilution method in the determination of cardiac output in clinical practice. Am Rev Respir Dis. 1982;126:1001–4.
25. Ngo C, Leonhardt S, Zhang T, Lüken M, Misgeld B, Vollmer T, et al. Linearity of electrical impedance tomography during maximum effort breathing and forced expiration maneuvers. Physiol Meas. 2017;38:77–86.
26. Frerichs I, Hahn G, Hellige G. Thoracic electrical impedance tomographic measurements during volume controlled ventilation-effects of tidal volume and positive end-expiratory pressure. IEEE Trans Med Imaging. 1999;18:764–73.
27. Michard F, Teboul J-L. Predicting fluid responsiveness in ICU patients. Chest. 2002;121:2000–8.
28. Grocott MPW, Hamilton MA. Resuscitation fluids. Vox Sang. 2002;82:1–8.
29. Braun F, Proença M, Adler A, Riedel T, Thiran J-P, Solà J. Accuracy and reliability of noninvasive stroke volume monitoring via ECG-gated 3D electrical impedance tomography in healthy volunteers. Tang D, editor. PLoS ONE. 2018;13:e0191870.
30. Patterson RP, Zhang J, Mason LI, Jerosch-Herold M. Variability in the cardiac EIT image as a function of electrode position, lung volume and body position. Physiol Meas. 2001;22:159–66.
31. Mauri T, Eronia N, Turrini C, Battistini M, Grasselli G, Rona R, et al. Bedside assessment of the effects of positive end-expiratory pressure on lung inflation and recruitment by the helium dilution technique and electrical impedance tomography. Intensive Care Med. 2016;42:1576–87.
32. Hellige G, Hahn G. Cardiac-related impedance changes obtained by electrical impedance tomography: an acceptable parameter for assessment of pulmonary perfusion? Crit Care. 2011;15:430.
33. Adler A, Proença M, Braun F, Brunner J, Solà J. Origins of Cardiosynchronous Signals in EIT. EIT 2017. Dartmouth, USA: Zenodo; 2017. p. 73.
34. Borges JB, Suarez-Sipmann F, Bohm SH, Tusman G, Melo A, Maripuu E, et al. Regional lung perfusion estimated by electrical

impedance tomography in a piglet model of lung collapse. J Appl Physiol. 2012;112:225–36.
35. Nguyen DT, Jin C, Thiagalingam A, McEwan AL. A review on electrical impedance tomography for pulmonary perfusion imaging. Physiol Meas. 2012;33:695–706.
36. Frerichs I, Hinz J, Herrmann P, Weisser G, Hahn G, Quintel M, et al. Regional lung perfusion as determined by electrical impedance tomography in comparison with electron beam CT imaging. IEEE Trans Med Imaging. 2002;21:646–52.
37. Iotti GA, Braschi A, Brunner JX, Smits T, Olivei M, Palo A, et al. Respiratory mechanics by least squares fitting in mechanically ventilated patients: applications during paralysis and during pressure support ventilation. Intensive Care Med. 1995;21:406–13.
38. Graf M, Riedel T. Electrical impedance tomography: amplitudes of cardiac related impedance changes in the lung are highly position dependent. Tolkacheva E, editor. PLOS ONE. 2017;12:e0188313.